



Experiment title:
**Non-equilibrium laser driven thermal crystallization
of the Si-Ge-Sn system
studied by (diffraction) imaging methods**

**Experiment
number:**
MA-3477

Beamline:
ID19

Date of experiment:
from: 17. May 2017 to: 21. May 2017

Date of report:
26. Feb. 2018

Shifts:
12

Local contact(s):
Alexander Rack & Margie Olbinado

Received at ESRF:

Names and affiliations of applicants (* indicates experimentalists):

Jörg Grenzer*, **Lars Rebohle**

Helmholtz-Zentrum Dresden-Rossendorf e.V., Institute of Ion Beam Physics and Materials
Research, Dresden, Germany

Andreas N. Danilewsky*, **Simon Bode***, **Simon Haaga***, **Merve Pinar Kabukcuoglu***

Kristallographie, Institut für Geo- und Umweltnaturwissenschaften

Albert-Ludwigs-Universität Freiburg, Germany

Report:

Si-Ge-Sn based heterostructures are the key material for the operation of Si photonic devices in the “new”, extended wavelength range from 1550 nm to 5000 nm. The present crystalline quality, however, is not sufficient for device operation. Lasers may be the solution to tackle these challenges. During a highly intense ns laser pulse, a near-surface layer liquefies whereas the bulk substrate remains at ambient temperature. The molten layer cools down and recrystallizes forcing atoms to remain at their actual position rebuilding the host lattice. If the process can be controlled, a bottom-up liquid phase epitaxial and the regrowth of a single crystalline layer takes place. Any presence of inhomogeneities disrupts the growth front and leads to the formation of defect rich or even poly-crystalline structures. Figure 1 shows the principal layout of the experiment: This experimental set-up was already successfully used and published in [1]. But, a different laser was used: A Nd:YAG (BrilliantB, Quantel, France; wavelength = 532 nm; ~5 ns; energy = 800 mJ).

We were not able to observe the formation of a diffraction peak, in-situ, during or right after a single laser shot.

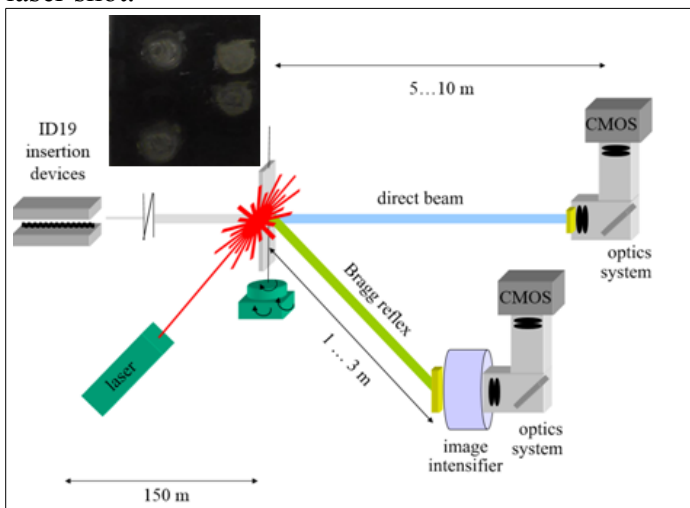


Figure 1: The experimental setup used during the experiment MA-377; laser and x-ray beam are perpendicular. The inset shows the effect of different laser shots at the sample varying the pulse energy. A detailed description can be found in [1]

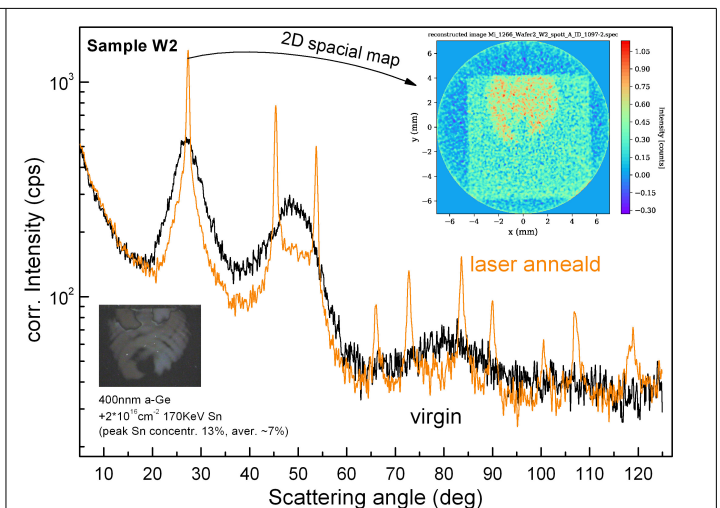


Figure 2: Laser driven crystallization of an amorphous Ge-Sn thin film: Ex-situ XRD (before, after a single shot (~0.01 J/mm²); insets: microscopic image (left) and a tomographic reconstruction (right) of the Ge-Sn (111) spatial distribution.

However using sufficient low laser powers ($\sim 0.01 \text{ J/mm}^2$ at $\sim 5 \text{ ns}$) a post ex-situ experiment has shown that the amorphous Ge(Sn) thin film under goes a crystallization process forming a homogeneous polycrystalline $\text{Sn}_{0.03}\text{Ge}_{0.97}$ thin film with a crystallite size of $\sim 10 \text{ nm}$. Figure 2 shows the X-ray diffraction signal of the pristine amorphous film and after the single shot laser annealing. The left inset shows a microscopy image; the recrystallized layer demonstrates a metallic behavior, whereas the amorphous film is always black. The right inset shows the corresponding spatial reconstruction of the GeSn (111) diffraction peak, which peak intensity is higher than the signal from the amorphous region.

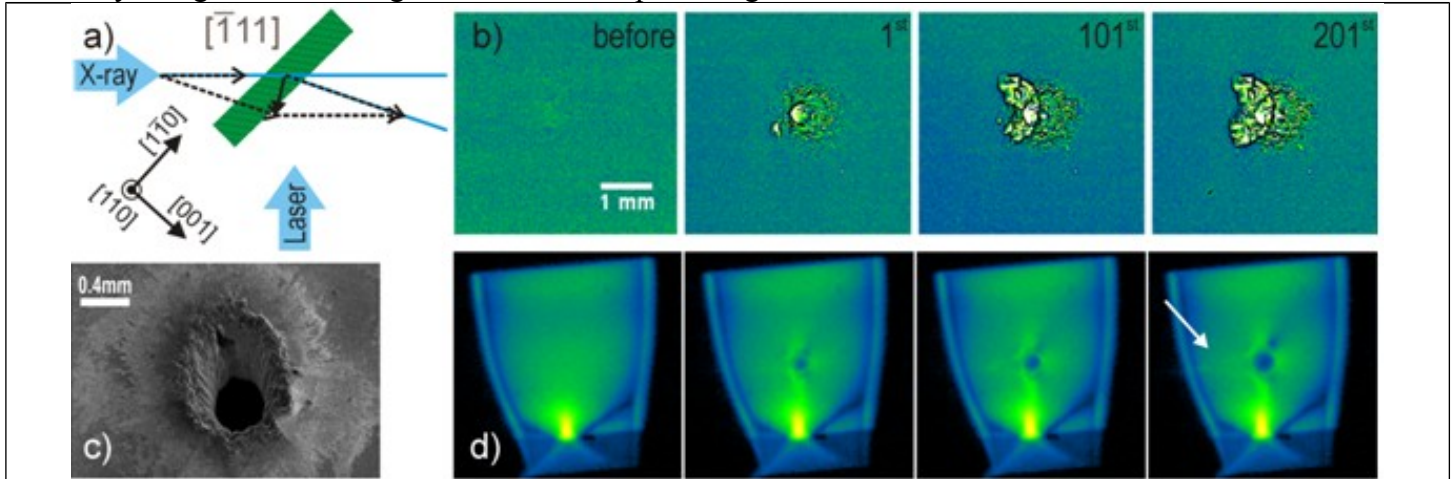


Figure 3: a) Schematic diagram of Si wafer orientation with respect to the laser and X-ray beams. The sample was placed by about 45° with respect to the laser and the X-ray beam. The laser was operated at maximum power at $\sim 1 \text{ J}$; the light was directed to the sample using a focusing lens resulting in a diameter of $\sim 0.3 \text{ mm}$. The X-ray beam size was about $12 \times 12 \text{ mm}^2$ to fully illuminate the $10 \text{ mm} \times 10 \text{ mm}$ wafer. The Bragg diffraction angle was tuned so that the Si (333) reflection (transmission geometry) was recorded by the diffraction topography detector. The transmission image (an area of $4 \times 4 \text{ mm}^2$ around the evolving hole is depicted) shown in b) was recorded with a frame rate of 3kfps (pco.dimax (PCO AG, Germany), Hasselblad tandem $f=100 \text{ mm}$, LYSO:Ce scintillator). The propagation distance between the sample and the detector was 7 m. The diffracted image shown in d) was recorded at a scattering angle of 19° , at 75 kfps (FASTCAM SA1.1, Photron Ltd., Japan); the sample detector distance was about 1.5 m. An SEM image of the laser impact is shown in c).

However, using phase-contrast radiography and diffraction topography we could record time resolved effects of ablation and the strain evolution during material removal. Whereas the material removal can be deduced from XPCI; information on the level of the atomic lattice can be obtained by using X-ray diffraction (XRD). Employing conventional CMOS cameras, we present in Figure 3 a simultaneous XPCI and diffraction topography experiment drilling a hole in a 0.50 mm thick single crystalline silicium wafer using a pulsed nanosecond laser. Figure 3a shows the orientation of the Si (001) wafer with respect to the laser and X-ray beams. Figure 3b and 3d demonstrate a series of XPCI images and the corresponding evolution of the Si (333) reflection during the initial stage of the hole formation (see Fig. 3c), i.e. before, after the 1st; the 101st and 201st laser shot, respectively. The response of the sample was recorded for 300 ms every 10 seconds (an equivalent to 100 laser shots), for about 120sec. In figure 3d the strain distribution is shown. To keep the sample in place during the process of laser drilling it was clamped with a plastic screw. Consequently, due to the point load of the screw a static strain pattern in the sample appeared causing an orientation contrast with a strong intensity modulation. The larger part of the sample shows a flat intensity distribution demonstrating an almost defect free material.

Within the 1st laser impact a hole start to be develop. Synchronously, in the diffraction image an additional strain feature with a circular shape in its center appeared that increases as the hole grew with drilling. Its extended shape resembles a threefold symmetry that coincides with the forward laser pressure and it spans a much larger area than the size of the physically drilled hole (arrow in fig. 3d). Interestingly, the intensity modulation (that could be understood as a measure for strength of the strain) is much weaker than the one that is caused by the clamping screw. Figure 3c shows that the removal of material is accompanied with the growth of a crater like wall structure at the border of the hole letting us conclude that the laser-sample interaction is mainly governed by a thermal process.

References:

- [1] M. P. Olbinado, V. Cantelli, O. Mathon, S. Pascarelli, J. Grenzer, A. Pelka, M. Roedel, I. Prencipe, A. Laso Garcia, U. Helbig, D. Kraus, U. Schramm, T. Cowan, M. Scheel, P. Pradel, T. De Resseguier and A. Rack, *J. Phys. D: Appl. Phys.* **51**, 055601 (2018).
- [2] M.P. Olbinado, J. Grenzer, P. Pradel, T. De Resseguier, P. Vagovic, M.C. Zdora, V.A. Guzenko, C. David, A. Rack, *Journal of Instrumentation*, submitted, (2018).